

1 Article

2 Analyze PFG Anomalous Diffusion via Real Space 3 and Phase Space Approaches

4 Guoxing Lin ^{1,*}

5 ¹ Carlson School of Chemistry and Biochemistry, Clark University, Worcester, MA 01610, USA

6 * Correspondence: glin@clarku.edu; Tel.: +1-508-793-7594

7 **Abstract:** Pulsed-field gradient (PFG) diffusion experiments can be used to measure anomalous
8 diffusion in many polymer or biological systems. However, it is still complicated to analyze PFG
9 anomalous diffusion, particularly the finite gradient pulse width (FGPW) effect. In practical
10 applications, the FGPW effect may not be neglected such as in clinical diffusion magnetic resonance
11 imaging (MRI). Here, two significantly different methods are proposed to analyze PFG anomalous
12 diffusion: the effective phase shift diffusion equation (EPSDE) method and an observing the signal
13 intensity at the origin method. The EPSDE method describes the phase evolution in virtual phase
14 space, while the method to observe the signal intensity at the origin describes the magnetization
15 evolution in real space. However, these two approaches give the same general PFG signal
16 attenuation including FGPW effect, which can be numerically evaluated by a direct integration
17 method. The direct integration method is fast and without overflow. It is a convenient numerical
18 evaluation method for Mittag-Leffler function type PFG signal attenuation. The methods here
19 provide a clear view of spin evolution under field gradient, and their results will help the analysis
20 of PFG anomalous diffusion.

21 **Keywords:** PFG anomalous diffusion; fractional derivative; NMR; MRI

23 1. Introduction

24 Anomalous dynamic behavior exists in many polymer or biological systems [1,2,3,4,5]. These
25 systems often consist of various molecules such as macromolecules and small penetrant molecules
26 like water. These molecules often demonstrate anomalous dynamics behavior: their rotational motion
27 time constant usually obey a stretched exponential distribution, namely the Kohlrausch-Williams-
28 Watts (KWW) function distribution [6,7], and their translational diffusion jump time and jump length
29 could follow power law distributions [2]. Nuclear magnetic resonance (NMR) is one of the important
30 techniques to detect these anomalous dynamic behaviors. For instance, anomalous diffusion can be
31 detected by pulsed-field gradient (PFG) NMR experiments.

32 PFG diffusion NMR [8,9,10,11,12,13,14] has been a powerful tool to measure normal diffusion.
33 The history of using field gradient to measure diffusion can be tracked back to Hahn, who first
34 observed the influence of the molecule diffusion under gradient magnetic field upon echo amplitudes
35 in 1950 [16]. PFG diffusion measurements have broad applications in NMR and magnetic resonance
36 imaging (MRI) [12-15]. For instance, the water diffusion difference in different part of the brain can
37 be used as an important contrast factor to build imaging of acute stroke [15]. The PFG technique,
38 being an ultra-valuable tool for normal disunion, could play an increasingly important role in
39 monitoring anomalous diffusion occurring in many polymer and biological systems.

40 PFG anomalous diffusion [16,17,18,19,20,21,22] is different from PFG normal diffusion. Unlike
41 normal diffusion, anomalous diffusion has a non-Gaussian probability distribution [2,23], and its
42 mean square displacement is not linearly proportional to diffusion time [2]. These non-Gaussian
43 characteristics make it complicated to analyze PFG anomalous diffusion. Although PFG anomalous
44 diffusion can be approximately analyzed by traditional methods such as the apparent diffusion
45 coefficient method, PFG theories based on the fractional derivative could not only improve the

46 analyzing accuracy on diffusion domain size, diffusion constant and other variables [
47 [16,179,24,25,26,27], but also yield additional information such as the time derivative order α and
48 space derivative order β that are related with diffusion jump time and jump length distributions
49 determined by material properties.

50 Many efforts have been devoted to studying PFG anomalous diffusion based on fractional
51 calculus, which includes the propagator method [28], the modified-Bloch equation method [16,24,29],
52 the effective phase shift diffusion equation method [17], the instantaneous signal attenuation method
53 [25], the modified-Gaussian or non-Gaussian distribution method [26], etc. Additionally, PFG
54 anomalous diffusions in restricted geometries such as plate, sphere, and cylinder have been
55 investigated [27]. These theoretical methods analyze PFG anomalous diffusion from different angles.
56 Therefore, each of them can have its own advantages in handling certain types of PFG anomalous
57 diffusion. To better apply the PFG technique to study anomalous diffusion, it is still valuable to
58 develop new theoretical treatments for PFG anomalous diffusion.

59 In this paper, two methods based on the fractional derivative [1,2,5,30,31,32] are proposed to
60 give general analytical PFG signal attenuation expressions for anomalous diffusion. The first method
61 is the recently developed effective phase shift diffusion equation (EPSDE) method [17]. This method
62 describes the spin phase evolution by an effective phase diffusion process in virtual phase space [17].
63 Solving the effective phase shift diffusion equation gives valuable information about the phase
64 evolution process such as the phase probability distribution function and the moment of mean phase
65 displacement. While, other conventional methods are difficult to get these phase information, and
66 usually assume an approximate phase distribution such as Gaussian phase distribution [12]. In this
67 paper, it will be shown that a solvable PFG signal attenuation equation can be derived by applying
68 Fourier transform to the effective phase shift equation. The second method is to observe the signal
69 intensity at the origin method, which is an ultra-simple new method. For a homogeneous diffusion
70 spin system, although the magnetization amplitude attenuates because of the gradient magnetic field
71 effect, the phase of magnetization keeps constant at the origin of the gradient field. Such a specific
72 phase property is employed to derive a PFG signal attenuation equation in this paper. The above two
73 methods give the same signal attenuation equation, from which the general PFG signal attenuation
74 expression can be derived by the Adomian decomposition method [33,34,35,36,37]. Besides the
75 Adomian decomposition method, a direct integration method was proposed for the numerical
76 evaluation of the PFG signal attenuation, which is a fast and simple method. The results include finite
77 gradient pulse width (FGPW) effect [12-14], namely the signal attenuation during each gradient pulse
78 applying period. Theoretically, during a short gradient pulse the PFG signal attenuation can be
79 neglected; nevertheless, the gradient pulse used in a clinical MRI is usually long [15, 38].
80 Additionally, a longer gradient pulse allows the measuring of slower diffusion under the same
81 gradient maximum intensity, which matters in studying polymer and biological systems where the
82 molecule diffusion is often slow. Therefore, it needs to consider the FGPW effect in many real
83 applications. The two methods here give the same results on the FGPW effect. These results agree
84 with reported results from some other methods [17,25,26,] and the continuous time random walk
85 simulation [25,28]. Furthermore, PFG anomalous diffusion of intramolecular multiple quantum
86 coherence (MQC) is also discussed [26]. The MQC effect has the benefit to enhance the gradient effect
87 on PFG signal attenuation [39]. The two methods provide a compliment view of PFG anomalous
88 diffusion from both the real space and phase space.

89 2. Theory

90 2.1. The phase space method-the effective phase shift diffusion method

91 For the sake of simplicity, only one-dimensional anomalous diffusion is considered in this paper.
92 In PFG experiments, the field gradient pulse results in a time and space dependent magnetic field
93 $B(z,t) = B_0 + g(t) \cdot z$, where B_0 is the exterior magnetic field, z is the position, and $g(t)$ is the time-
94 dependent gradient [12-14]. The magnetic field exerts a torque on each spin moment. The torque
95 changes the spin angular momentum direction, which leads the spin to precess about the magnetic
96 field with Larmor frequency $\omega(z,t) = -\gamma B(z,t)$. In a rotating frame with angular frequency $\omega_0 = -\gamma B_0$

97 , a diffusing spin at position $z(t')$ has a time-dependent angular frequency $\gamma g(t') \cdot z(t')$, and its phase
 98 accumulated along the diffusion path is [12-14,18]

$$99 \quad \phi(t) = -\int_0^t \gamma g(t') \cdot z(t') dt', \quad (1)$$

100 where $\phi(t)$ is the net accumulating phase. The range of $\phi(t)$ is $-\infty < \phi(t) < \infty$ rather than
 101 $-\pi \leq \phi(t) \leq \pi$. $\cos(\phi(t))$ is the projection factor of the spin magnetization to the observing coordinate
 102 axis. The PFG signal comes from the ensemble contribution from all spins by averaging over all
 103 possible phases [12-14]:

$$104 \quad S(t) = S(0) \int_{-\infty}^{\infty} P(\phi, t) \exp(+i\phi) d\phi, \quad (2)$$

105 where $S(0)$ is the signal intensity at the beginning of the first gradient pulse, $S(t)$ is the signal
 106 intensity at time t , and $P(\phi, t)$ is the accumulating phase probability distribution function. In a
 107 symmetric diffusion system, Equation (2) can be further written as

$$108 \quad S(t) = S(0) \int_{-\infty}^{\infty} P(\phi, t) \cos(\phi) d\phi. \quad (3)$$

109 Because the NMR signal comes from numerous spins, the percentage of spins with potential infinite
 110 $\phi(t)$ is very small, which can thus be neglected. Additionally, $-1 \leq \cos(\phi(t)) \leq 1$, therefore,
 111 $0 \leq |S(t)| \leq |S(0)|$, and $S(t)$ is a finite quantity that can be measured in NMR experiments. A possible
 112 infinite "mean square phase displacement" $\langle |\phi(t)|^2 \rangle$ is not necessary an obstacle in PFG NMR
 113 measurement, although it may have a significant effect in other academic fields. The PFG signal
 114 attenuation can be obtained based on Equations (2) or (3), but the phase evolution process based on
 115 the phase path integral equation (1) is complicated. Nevertheless, the recently developed effective
 116 phase shift diffusion equation method provides a simple way to describe the phase evolution based
 117 on an effective phase diffusion process [17]. In the following, the effective phase diffusion equation
 118 method [17] will be briefly reintroduced. Additionally, a general solution including the finite gradient
 119 pulse width effect will be given that has not been reported in [17].

120 For simplicity, only the diffusion with symmetric probability distribution is studied here. The
 121 self-diffusion process can be described by a random walk, which consists of a sequence of
 122 independent random jumps with waiting times $\Delta t_1, \Delta t_2, \Delta t_3, \dots, \Delta t_n$, and corresponding
 123 displacement lengths $\Delta z_1, \Delta z_2, \Delta z_3, \dots, \Delta z_n$. Based on the random walk, Equation (1) can be
 124 rewritten as [17]

$$125 \quad \begin{aligned} \phi(t) &= -\sum_{i=1}^n \gamma \Delta t_i g(t_i) \cdot \left(\sum_{m=1}^i \Delta z_m + z_0 \right) \\ &= -\gamma \sum_{m=1}^n \left[\sum_{i=1}^n \Delta t_i g(t_i) - \sum_{i=1}^{m-1} \Delta t_i g(t_i) \right] \cdot \Delta z_m - \gamma \sum_{i=1}^n \Delta t_i g(t_i) \cdot z_0 \\ &= -\sum_{m=1}^n [K(t) - K(t_{m-1})] \cdot \Delta z_m - K(t) \cdot z_0 \\ &= -\sum_{m=1}^n [K(t) - K(t_m)] \cdot \Delta z_m - K(t) \cdot z_0 \end{aligned} \quad (4)$$

126 where

$$127 \quad K(t) = \int_0^t \gamma g(t') dt', \quad (5)$$

128 is the wavenumber [12-14]. In Equation (4), $K(t_m) \approx K(t_{m-1})$ is used because $[K(t_m) - K(t_{m-1})] \cdot \Delta z_m$ is
 129 neglectable, and the temporal and spatial summation orders are interchanged because $\Delta t_i g(t_i)$ and
 130 Δz_m are often non-correlated. In most PFG experiments, $K(t_{tot}) = 0$ where t_{tot} is the time at the end
 131 of the rephasing gradient pulse, so Equation (4) can be further simplified to [17]

$$132 \quad \phi(t_{tot}) = -\sum_m K(t_m) \cdot \Delta z_m. \quad (6)$$

133 The $-\sum_m K(t_m) \cdot \Delta z_m$ term in Equation (6) is an effective phase random walk with a jump length
 134 $-K(t_m) \cdot \Delta z_m$ and a jump waiting time Δt_m . The phase random walk can be treated as an effective
 135 phase diffusion, which can be obtained from the corresponding spin diffusion in the real space by
 136 scaling the jump length $\Delta z(t)$ by a factor $-K(t)$. Because $\langle |\Delta z|^\beta \rangle / \langle \Delta t^\alpha \rangle \propto D_f$ and
 137 $\langle |K(t)\Delta z|^\beta \rangle / \langle \Delta t^\alpha \rangle \propto D_{\text{eff}}(t)$, the effective phase diffusion constant is $D_{\text{eff}}(t) = K^\beta(t) D_f$ (oftentimes
 138 $K(t) \geq 0$) [17], where D_f and $D_{\text{eff}}(t)$ are the fractional diffusion coefficients for the real space
 139 diffusion and the effective phase diffusion respectively, and their units are m^β / s^α and $\text{rad}^\beta / s^\alpha$.
 140 As both the effective phase diffusion and the real spin particle diffusion belong to the same type
 141 diffusion, they should obey the same type diffusion equation. The one-dimensional real space
 142 diffusion equation based on the fractional derivative is [5,30-32]

$$143 \quad {}_t D_*^\alpha M_{xy}(z, t) = D_f \frac{\partial^\beta}{\partial |z|^\beta} M_{xy}(z, t), \quad (7)$$

144 where ${}_t D_*^\alpha$ is the Caputo fractional derivative defined as [5,30-32]

$$145 \quad {}_t D_*^\alpha f(t) := \begin{cases} \frac{1}{\Gamma(m-\alpha)} \int_0^t \frac{f^{(m)}(\tau) d\tau}{(t-\tau)^{\alpha+1-m}}, & m-1 < \alpha < m, \\ \frac{d^m}{dt^m} f(t), & \alpha = m. \end{cases}, \quad (8)$$

146 and $\frac{\partial^\beta}{\partial |z|^\beta}$ is the space fractional derivative [5,30-32] defined in Appendix A. By replacing coordinate
 147 z with ϕ , and D_f with $D_{\text{eff}}(t)$ respectively from real space diffusion equation (9), the effective
 148 phase diffusion equations can be obtained [17] as

$$149 \quad {}_t D_*^\alpha P(\phi, t) = K^\beta(t) D_f \frac{\partial^\beta}{\partial |\phi|^\beta} P(\phi, t). \quad (9)$$

150 As $\hat{F}(f(x, t)) = f(q, t)$ and $\hat{F}\left(\frac{\partial^\beta}{\partial |x|^\beta} f(x); q\right) = -q^\beta f(q)$ [30-32] where q is wavenumber,

151 applying Fourier transform $\hat{F}f(x) = \int_{-\infty}^{\infty} f(x) \exp(+iqx) dx$ on both sides of Equation (9) gives

$$152 \quad {}_t D_*^\alpha P(q, t) = -K^\beta(t) q^\beta D_f P(q, t), \quad (10)$$

153 which is a q space phase diffusion equation. Here, q is the wavenumber dedicated to the above
 154 Fourier transform, which differs from the field gradient pulse induced wavenumber $K(t)$ defined
 155 by Equation (5). When $q = 1$, $P(q, t)$ in Equation (10) equals the attenuated signal amplitude because
 156 in PFG experiments the signal attenuation can be calculated based on Equation (2) as [17]

$$157 \quad S(t) = S(0) \int_{-\infty}^{\infty} P(\phi, t) \exp(+i\phi) d\phi = p(1, t). \quad (11)$$

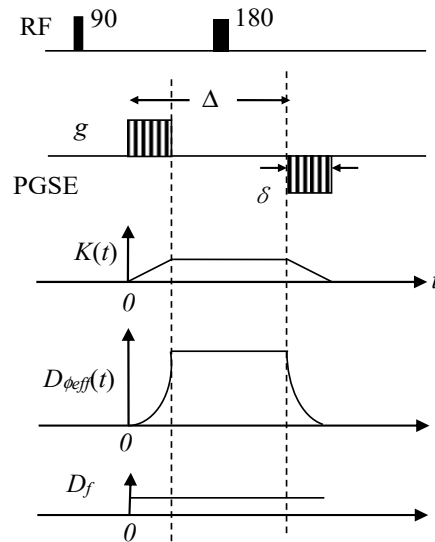
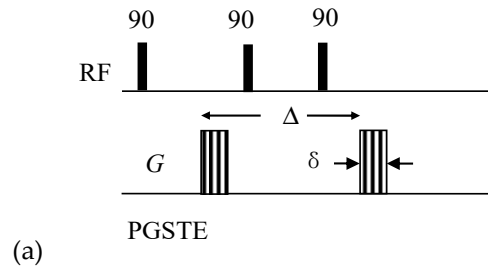
158 The normalized value of $S(0)$ equaling 1 will be used and dropped out throughout this paper.
 159 Substituting Equation (11) and $q = 1$ into Equation (10), we get

$$160 \quad {}_t D_*^\alpha S(t) = -D_f K^\beta(t) S(t), \quad (12)$$

161 which is the PFG signal attenuation equation.

162 The solution of Equation (12) will be given in section 2.3 as the same equation will be obtained
 163 by the observing the signal intensity at the origin method in the subsequent section.

164



165

(b)

166

Figure 1. (a) PGSTE pulse sequences; (b) PGSE pulse sequence. The gradient pulse width is δ , and the diffusion delay is Δ . The time-dependent behavior of wavenumber $K(t)$, diffusion constant D_f , and the effective phase diffusion constant $D_{\phi_{eff}}(t) = K^\beta(t)D_f$ is also demonstrated below PGSE pulse sequence.

167

168

169

170

171

172

173

2.2 Observing the signal intensity at the origin in real space

174

For a non-diffusing spin, in a rotating frame with angular frequency $\omega_0 = -\gamma B_0$, its precession phase can be described as [12-14]

175

$$\psi(z,t) = (\omega - \omega_0)t = -K(t) \cdot z, \quad (13)$$

176

where $\psi(z,t)$ is the precession phase, which is different from the accumulated phase $\phi(t)$ described by (1). The non-diffusing spin system has a time and space modulated magnetization, which can be described as

177

$$M_{xy}(z,t) = S(t) \exp(-iK(t) \cdot z), \quad (14)$$

178

where $S(t)$ is the magnetization amplitude which can be referred to as signal intensity, and the $\exp(-iK(t) \cdot z)$ is the phase term. For a pulsed gradient spin echo (PGSE) or the pulsed gradient stimulated-echo (PGSTE) experiment with a constant gradient as shown in Figure 1, the wavenumber

179

180

181

182

183

184

185

$$K(t) = \begin{cases} \gamma g t, 0 < t \leq \delta, \text{dephasing gradient} \\ \gamma g \delta, \delta < t \leq \Delta \\ \gamma g (\Delta + \delta - t), \Delta < t \leq \Delta + \delta, \text{rephasing gradient} \end{cases}, \quad (15)$$

186 where δ is the gradient pulse length, and Δ is the diffusion delay starting from the beginning of
 187 the first dephasing gradient pulse to the end of the last rephrasing gradient pulse. Because of the two
 188 counteracting gradient pulses—a dephasing pulse and a rephrasing pulse, $K(t)$ returns to 0 at the end
 189 of the rephrasing pulse, and the phase of non-diffusing spins will be refocused. Therefore, the signal
 190 of the non-diffusing spin system does not attenuate, when the T_2 relaxation is neglected.

191 For the spin diffusion in a homogeneous sample, its magnetization still can be described by
 192 Equation (14), $M_{xy}(z, t) = S(t) \exp(-iK(t) \cdot z)$. At a random position z , the possibilities of spins
 193 diffusing to opposite directions $z \pm \Delta z$ are equal [25]. The opposite movements yield
 194 $\exp(-iK(t) \cdot (z + \Delta z)) + \exp(-iK(t) \cdot (z - \Delta z)) = \cos(K(t) \cdot \Delta z) \exp(-iK(t) \cdot z)$, which has no effect on the
 195 phase, $\exp(-iK(t) \cdot z)$, but does make the signal intensity decay by a factor $\cos(K(t) \cdot \Delta z)$ for these
 196 spins. By substituting $M_{xy}(z, t) = S(t) \exp(-iK(t) \cdot z)$ into diffusion Equation (7), and applying

197 $\frac{\partial^\beta}{\partial |z|^\beta} \exp(-iK(t) \cdot z) = -K^\beta(t) \exp(-iK(t) \cdot z)$, we have

$$198 \quad {}_t D_*^\alpha [S(t) \exp(-iK(t) \cdot z)] = -D_f K^\beta(t) [S(t) \exp(-iK(t) \cdot z)]. \quad (16)$$

199 At the origin, $z = 0$, $i\gamma z = 0$, $\exp(-iK(t) \cdot z) = 1$, and $S(t) \exp(-iK(t) \cdot z) = S(t)$, we thus have

$$200 \quad {}_t D_*^\alpha S(t) = -D_f K^\beta(t) S(t). \quad (17)$$

201 Equation (17) is identical to Equation (12) obtained by the effective phase shift diffusion equation
 202 method in the previous section 2.1.

203 This observing signal intensity at the origin method could be understood in another way: if only
 204 the signal intensity or amplitude is observed from a selected position at different diffusion time
 205 $t_i, i = 1, 2, 3, \dots$ in a PFG anomalous diffusion experiment, the observed signal intensity or amplitude
 206 shall still obey Equation (17) regardless whether the phase is observed or not. It is reasonable that
 207 both ways can give the same signal attenuation expression, because the signal amplitude is
 208 homogeneous throughout the sample at each instant, and selecting the origin at a random position
 209 in the sample does not affect the result.

210 2.3. Analytical solution by the Adomian decomposition method

211 The same equation as Equation (12) or (17) has been obtained by the fractional integral modified-
 212 Bloch equation method. The three different methods get the same PFG signal attenuation equation.
 213 Reference [29] has employed the Adomian decomposition method to give a general analytical
 214 solution to Equation (12). In the following, the general solution from the Adomian decomposition
 215 will be given in more detail for the cases of normal diffusion and general anomalous diffusion.

216 2.3.1 normal diffusion.

217 First, the signal attenuation equation, Equation (12) or (17) can be used to obtain the PFG signal
 218 attenuation expression for normal diffusion, which is a specific case of anomalous diffusion with
 219 $\alpha = 1$ and $\beta = 2$. When $\alpha = 1$ and $\beta = 2$, Equation (17) reduces to

$$220 \quad \frac{d}{dt} S(t) = -K^2(t) D S(t), \quad (18)$$

221 where D is the diffusion constant of normal diffusion. The solution of Equation (18) is

$$222 \quad S(t) = \exp\left(-\int_0^t D K^2(t') dt'\right), \quad (19)$$

223 which is the PFG signal attenuation expression for normal diffusion. The same result as expression
 224 (19) has been obtained in [40]. For PGSE or PGSTE experiments, the PFG signal attenuation calculated
 225 based on Equation (19) is $\exp(-D_{f1} \gamma^2 g^2 \delta^2 (\Delta - \delta/3))$, which is a routinely used expression for PFG
 226 normal diffusion [12-14].

227 2.3.2 general anomalous diffusion.

228 Second, the PFG signal attenuation for general anomalous diffusion can be obtained. The same
 229 equation as Equation (17) and its solution have been obtained by modified-Bloch equation method in
 230 [29]. According to [29], Equations (12) or (17) can be written equivalently as

$$231 \quad S(t) = \sum_{k=0}^{m-1} S^{(k)}(0^+) \frac{t^k}{k!} + J^\alpha(a(t)S(t)), m-1 < \alpha < m, \quad (20)$$

232 where

$$233 \quad a(t) = -K^\beta(t)D_f = \begin{cases} -(\gamma g t)^\beta D_f, 0 < t \leq \delta \\ -(\gamma g \delta)^\beta D_f, \delta < t \leq \Delta \\ -(\gamma g)^\beta (\Delta + \delta - t)^\beta D_f, \Delta < t \leq \Delta + \delta \end{cases}. \quad (21)$$

234 Based on the Adomian decomposition method [33-37], the solution of Equation (20) is [29]

$$235 \quad S(t) = \sum_{n=0}^{\infty} S_n(t), \quad (22a)$$

236 where

$$237 \quad S_0(t) = \sum_{k=0}^{m-1} S^{(k)}(0^+) \frac{t^k}{k!}, m-1 < \alpha < m, \quad (22b)$$

238 and

$$239 \quad \begin{aligned} S_n(t) &= J^\alpha(a(t)S_{n-1}(t)) \\ &= -\int_0^t \frac{(t-\tau)^{\alpha-1}}{\Gamma(\alpha)} D_f K^\beta(\tau) S_{n-1}(\tau) d\tau. \\ &= -\int_0^t \frac{D_f K^\beta(\tau) S_{n-1}(\tau) d(t-\tau)^\alpha}{\alpha \Gamma(\alpha)} \end{aligned} \quad (22c)$$

240 In PGSE or PGSTE experiments, the time t can be separated into three periods: $0 < t \leq \delta$,
 241 $\delta < t \leq \Delta$, $\Delta < t \leq \Delta + \delta$. If the initial condition, $S^{(1)}(0^+) = 0$, is used [30-32] for a free diffusion in a
 242 homogeneous sample, we can get the following:

243 (a) *PFG signal attenuation under SGP approximation*: δ is short enough and the diffusion inside
 244 each gradient pulse can be neglected. We get

$$245 \quad S(\Delta) = \sum_{n=0}^{\infty} S_n(\Delta) = E_{\alpha,1}(-D_f K_{SGP}^\beta \Delta^\alpha), K_{SGP} = \gamma g \delta, \quad (23)$$

246 where $S_0(\Delta) = 1$, and $S_n(\Delta) = \frac{(-D_f (\gamma g \delta)^\beta \Delta^\alpha)^n}{\Gamma(1+n\alpha)}$. Equation (23) replicates the SGP
 247 approximation result obtained in references [17,25,26].

248 (b) *Single pulse attenuation*: this is an ideal situation, the first gradient pulse is regular, but the
 249 second gradient pulse is infinitely narrow whose purpose is to counteract the first gradient
 250 pulse. We get

$$251 \quad \begin{aligned} S(t) &= \sum_{n=0}^{\infty} S_n(t) = 1 + \sum_{n=0}^{\infty} \left(-D_f (\gamma g)^\beta t^{(\alpha+\beta)}\right)^n \prod_{k=1}^n \frac{\Gamma(1+(k-1)\alpha+n\beta)}{\Gamma(1+k(\alpha+\beta))}, \\ &= E_{\alpha,1+\beta/\alpha,\beta/\alpha}(-D_f (\gamma g)^\beta t^{\alpha+\beta}) \end{aligned} \quad (24)$$

252 where $S_0(t) = 1$, $S_n(t) = \left(-D_f (\gamma g)^\beta t^{(\alpha+\beta)}\right)^n \prod_{k=1}^n \frac{\Gamma(1+(k-1)\alpha+n\beta)}{\Gamma(1+k(\alpha+\beta))}$, and

253 $E_{\alpha,\eta,\gamma}(x) = \sum_{n=0}^{\infty} c_n x^n$, $c_0 = 1$, $c_n = \prod_{k=0}^{n-1} \frac{\Gamma((k\eta+\gamma)\alpha+1)}{\Gamma((k\eta+\gamma+1)\alpha+1)}$ is a Mittag-Leffler type function [41].

254 Equation (24) is consistent with the results obtained by the modified Bloch equation
 255 proposed in [24]

256 (c) *General PFG signal attenuation*: the PGSE or PGSTE experiment includes three periods:
 257 $0 < t_1 \leq \delta$, $\delta < t_2 \leq \Delta$, and $\Delta < t_3 \leq \Delta + \delta$. The integration in Equation (22c) during these
 258 three periods is tedious, which can be calculated with computer assistance. Nevertheless,
 259 we can get the first and second terms of Equation (22a) as the following:

$$260 \quad S_0(t) = 1, \quad (25a)$$

261
262
263

$$S_1(t) = J^\alpha(a(t)S_0(t)) = -\int_0^t \frac{(t-\tau)^{\alpha-1}}{\Gamma(\alpha)} D_f K^\beta(\tau) d\tau = -\frac{D_f(\gamma g)^\beta}{\Gamma(1+\alpha)} \times$$

264

$$\left\{ \begin{array}{l} \alpha^{\alpha+\beta} B(\beta+1, \alpha), \quad 0 < t \leq \delta \\ \alpha^{\alpha+\beta} \left[B(\beta+1, \alpha) - B\left(\frac{\delta}{t}; \beta+1, \alpha\right) \right] - \delta^\beta (t-\delta)^\alpha, \quad \delta < t \leq \Delta \\ \left\{ \alpha^{\alpha+\beta} \left[B(\beta+1, \alpha) - B\left(\frac{\delta}{t}; \beta+1, \alpha\right) \right] - \delta^\beta [(t-\delta)^\alpha - (t-\Delta)^\alpha] \right\} - \\ \int_\Delta^t \alpha(t-\tau)^{\alpha-1} (\Delta+\delta-\tau)^\beta d\tau, \quad \Delta < t \leq \Delta+\delta \end{array} \right. , \quad (25b)$$

265
266

where $B(x,y)$ and $B(a;x,y)$ are the Beta function and incomplete Beta function. When $t = \Delta + \delta$, Equation (25b) gives

267

$$\begin{aligned} S_1(\Delta + \delta) &= J^\alpha(a(t)S_0(t)) \\ &= -\int_0^{\Delta+\delta} \frac{(\Delta+\delta-\tau)^{\alpha-1}}{\Gamma(\alpha)} D_f K^\beta(\tau) d\tau \quad . (26) \\ &= -\frac{D_f(\gamma g)^\beta}{\Gamma(1+\alpha)} \left\{ \alpha(\Delta+\delta)^{\alpha+\beta} \left[B(\beta+1, \alpha) - B\left(\frac{\delta}{\Delta+\delta}; \beta+1, \alpha\right) \right] + \delta^\beta (\Delta^\alpha - \delta^\alpha) + \frac{\alpha \delta^{\alpha+\beta}}{(\alpha+\beta)} \right\} \end{aligned}$$

268

269

Equation (26) agrees with the signal attenuation expression $S(t) = E_{\alpha,1} \left(-\int_0^t D_f K^\beta(t') dt'^\alpha \right)$

270

obtained by the instantaneous signal attenuation method [25]. At small signal attenuation,

271

$S(t) = E_{\alpha,1} \left(-\int_0^t D_f K^\beta(t') dt'^\alpha \right)$ can be approximately expanded as

272

$$\begin{aligned} S(t) &= E_{\alpha,1} \left(-\int_0^t D_f K^\beta(t') dt'^\alpha \right) \\ &\approx 1 - \frac{D_f(\gamma g)^\beta}{\Gamma(1+\alpha)} \left\{ \alpha(\Delta+\delta)^{\alpha+\beta} \left[B(\alpha, \beta+1) - B\left(\frac{\Delta}{\Delta+\delta}; \alpha, \beta+1\right) \right] + \delta^\beta (\Delta^\alpha - \delta^\alpha) + \frac{\alpha \delta^{\alpha+\beta}}{(\alpha+\beta)} \right\} \cdot (27) \end{aligned}$$

273

274

Equation (27) is the same as that given by the combination of Equations (25a) and (26) (Note $B(x,y) = B(y,x)$ and $B(a;x,y) = B(1-a;y,x)$), however, at large signal attenuation,

275

276

$E_{\alpha,1} \left(-\int_0^t D_f K^\beta(t') dt'^\alpha \right)$ may deviate from the combination of Equations (25a) and (26) as

277

278

279

the higher order terms in the expansion cannot be omitted. This agreement can be explained by the following: in typical PGSE or PGSTE experiments, both the gradient intensity and pulse length of the dephasing pulse and the rephrasing pulse are identical, $|g_1| = |g_2|$ and

280

$\delta_1 = \delta_2$, thus $K(\Delta + \delta - \tau) = K(\tau)$ which results in

281

$$\begin{aligned} -\int_0^{\Delta+\delta} \frac{(\Delta+\delta-\tau)^{\alpha-1}}{\Gamma(\alpha)} D_f K^\beta(\tau) d\tau &\xrightarrow{\tau=\Delta+\delta-\tau'} = -\int_0^{\Delta+\delta} \frac{\tau'^{\alpha-1}}{\Gamma(\alpha)} D_f K^\beta(\Delta+\delta-\tau') d\tau' \\ &\xrightarrow{K(\Delta+\delta-\tau')=K(\tau')} = -\int_0^{\Delta+\delta} \frac{\tau'^{\alpha-1}}{\Gamma(\alpha)} D_f K^\beta(\tau') d\tau' \quad . (28) \end{aligned}$$

282 When $0 < \alpha \leq 2, \beta = 2$, the general anomalous diffusion reduces to time-fractional diffusion and
 283 Equation (25b) can be further calculated as

$$284 \quad S_1(\Delta + \delta) = -\frac{D_f(\mathcal{I}_g)^2}{\Gamma(1+\alpha)} \times \left\{ \frac{\alpha \delta^{\alpha+2}}{(\alpha+2)} + \delta^2(\Delta^\alpha - \delta^\alpha) + \frac{2}{(\alpha+1)(\alpha+2)} [(\Delta + \delta)^{2+\alpha} - \Delta^{2+\alpha}] - \frac{2}{(\alpha+1)} \Delta^{1+\alpha} \delta - \Delta^\alpha \delta^2 \right\}. \quad (29)$$

285 When $\alpha = 1, 0 < \beta \leq 2$, the general anomalous diffusion reduces to space-fractional diffusion.

286 Equation (22) reduces to $S(t) = \exp\left(-\int_0^t DK^\beta(t')dt'\right)$, which is the same as that obtained by [17,25,29].

287
 288 *2.4. Numerical evaluation of Mittag-Leffler function based PFG signal attenuation by the direct integration*
 289 *method*

290 Although the Adomian decomposition method can be used to numerically evaluate the PFG
 291 signal attenuation, its calculation speed is slow and it could cause overflow at large signal
 292 attenuation. References [29, 42] proposed an alternative method, a direct integration method that
 293 can give the same numerical results, but with a much fast speed and without overflow. From

294 Equation (20), if we set $\sum_{k=0}^{m-1} S^{(k)}(0^+) \frac{t^k}{k!} = 1$, we have

$$295 \quad S(t) = 1 - \int_0^t \left\{ \frac{(t-\tau)^{\alpha-1}}{\Gamma(\alpha)} G(\tau) \right\} S(\tau) d\tau, \quad (30)$$

296 where $G(t) = K^\beta(t)D_f$. If we denote $E_{\alpha,1,G(t)}(-t) = s(t)$, Equation (30) can be further written as

$$297 \quad E_{\alpha,1,G(t)}(-t) = 1 - \int_0^t \left\{ \frac{(t-\tau)^{\alpha-1}}{\Gamma(\alpha)} G(\tau) \right\} E_{\alpha,1,G(t)}(-\tau) d\tau. \quad (31a)$$

298 When $G(t) = 1$, $E_{\alpha,1,G(t)}(-t) = E_{\alpha,1}(-t^\alpha)$, which is a Mittag-Leffler function; when $G(t) = c, c > 0$,
 299 $E_{\alpha,1,G(t)}(-t) = E_{\alpha,1}(-ct^\alpha)$. Hence, we have

$$300 \quad E_{\alpha,1}(-t^\alpha) = 1 - \int_0^t \left\{ \frac{(t-\tau)^{\alpha-1}}{\Gamma(\alpha)} \right\} E_{\alpha,1}(-\tau^\alpha) d\tau, \quad (31b)$$

$$301 \quad E_{\alpha,1}(-ct^\alpha) = 1 - \int_0^t \left\{ \frac{(t-\tau)^{\alpha-1}}{\Gamma(\alpha)} c \right\} E_{\alpha,1}(-c\tau^\alpha) d\tau. \quad (31c)$$

302 Equation (30) can be rewritten in a discrete form as

$$303 \quad S(t_j) = 1 - \sum_{k=1}^j a(t_k) S(t_{k-1}) [(t_j - t_{k-1})^\alpha - (t_j - t_k)^\alpha] / \Gamma(1+\alpha). \quad (32)$$

304 where $t_j = \sum_{k=1}^j \Delta t_k$. Based on Equation (32), the PFG signal attenuation $S(t_1), S(t_2), \dots, S(t_n)$ can be
 305 calculated step by step starting from $S(t_1)$ to $S(t_n)$. Similarly, the Mittag-Leffler type function and
 306 its derivative can be numerically evaluated by:

$$307 \quad E_{\alpha,1,G(t)}(-t_j) = 1 - \sum_{k=1}^j G(t_k) E_{\alpha,1,G(t)}(t_{k-1}) [(t_j - t_{k-1})^\alpha - (t_j - t_k)^\alpha] / \Gamma(1+\alpha), \quad (33)$$

$$308 \quad E'_{\alpha,1,G(t)}(-t_j) = \frac{[E_{\alpha,1,G(t)}(-t_j) - E_{\alpha,1,G(t)}(-t_{j-1})]}{\Delta t_j}. \quad (34)$$

309 This method is simple, and it has no overflow issue in the calculation.

310
 311

312 3. CTRW in a lattice model

313 Random walk simulation is a powerful numerical method that employs a stochastic jump
 314 process to model normal and anomalous diffusion in physics, chemistry, biology and many other
 315 disciplines. It can be used to simulate the PFG signal attenuation in mathematically tractable or
 316 intractable systems. In this paper, the CTRW simulation method developed in [25] is used to verify
 317 the theoretical results, which is based on two models: the CTRW model [43] and the Lattice model
 318 [44,45]. In the simulation, a sequence of independent random waiting time and jump length
 319 combinations $(\Delta t_1, \Delta \xi_1), (\Delta t_2, \Delta \xi_2), (\Delta t_3, \Delta \xi_3), \dots, (\Delta t_n, \Delta \xi_n)$ is produced by computer program.
 320 The individual waiting time Δt and jump length $\Delta \xi$, are given according to [25] by the following
 321 expressions:

$$322 \quad \Delta t = -\eta_t \log U \left(\frac{\sin(\alpha\pi)}{\tan(\alpha\pi V)} - \cos(\alpha\pi) \right)^{\frac{1}{\alpha}}, \quad (35)$$

323 and

$$324 \quad \Delta \xi = \eta_z \left(\frac{-\log U \cos(\Phi)}{\cos((1-\beta)\Phi)} \right)^{\frac{1}{\beta}} \frac{\sin(\beta\Phi)}{\cos(\Phi)}, \quad (36)$$

325 where η_t and η_z are scale constants, $\Phi = \pi(V - 1/2)$, and $U, V \in (0,1)$ are two independent random
 326 numbers. The CTRW simulation based on the above waiting time and jump length satisfies the time-
 327 space fractional diffusion equation under the diffusive limit, which provides a simple way to simulate
 328 anomalous diffusion in various research areas, such as physics, and economics [43].

329 Although continuous waiting time and jump length are used in the simulation, the accumulating
 330 spin phase associated with the diffusion path is recorded in a discrete manner. Such a discrete phase
 331 recording manner is convenient and reasonable. The simulation can be viewed as a numerical pulsed-
 332 field gradient experiment, whose observables such as phase can be observed in a discrete time
 333 selected by an experiment observer; the observing or recording manner will not affect the
 334 fundamental numerical experiment process, namely the producing of the continuous random walk
 335 sequence: $(\Delta t_1, \Delta \xi_1), (\Delta t_2, \Delta \xi_2), (\Delta t_3, \Delta \xi_3), \dots, (\Delta t_n, \Delta \xi_n)$. The spin phase was recorded by the
 336 lattice model developed in [27,28], which has been applied to simulate PFG diffusion in polymer
 337 system [46]. The spin phase in the simulation is

$$338 \quad \phi(t'_j) = \sum_{j=1}^l \gamma \xi(t_j) \xi(t_j) \Delta t_j + \gamma \xi(t_l) (t'_j - t_l), \quad t_l \leq t'_j \leq t_{l+1}, \quad (37)$$

339 where $t_l = \sum_{j=1}^l \Delta t_j$, $\xi(t_l) = \sum_{j=1}^l \Delta \xi_j$, and t'_j is the discrete record time, which takes place between the l^{th}

340 and $l+1^{\text{th}}$ steps of the random walk. The second term $\gamma \xi(t_l) (t'_j - t_l)$ on the right-hand side of
 341 Equation (37) corresponds to the partial phase evolution of the $l+1^{\text{th}}$ jump step that needs to be
 342 recorded at the time t'_j . The PFG signal attenuation in the simulation can be obtained by averaging
 343 over all the walkers in the simulation [25,45,46]

$$344 \quad S(t) = \langle \cos[\phi_i(t)] \rangle = \frac{1}{N_{walks}} \sum_{i=1}^{N_{walks}} \cos[\phi_i(t)], \quad (38)$$

345 where N_{walks} is the total number of the walks. The total walks in each simulation are 1,000,000.

346 Because the CTRW model proposed in [25] is only for subdiffusion, the simulation here is limited
 347 to the subdiffusion. Interested readers are referred to references [25,29,43-46] for more detailed
 348 information.

349 4. Results and discussion

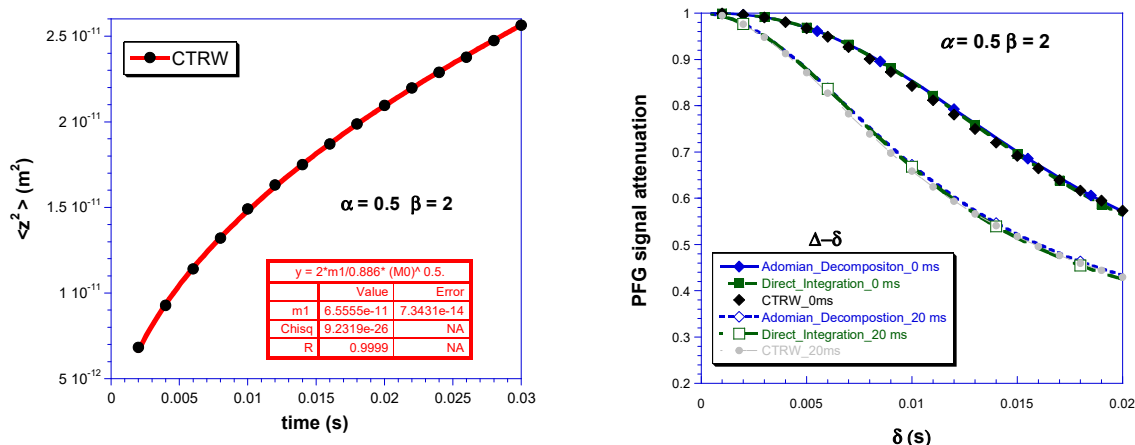
350 **Table 1.** Comparison PFG anomalous diffusion results by the effective phase shift diffusion method, the
 351 observing the signal intensity at the origin method and other methods.

Virtual phase space diffusion	Real space spin diffusion
Effective phase shift diffusion equation	Observing the signal intensity at the origin

366 These two approaches view the spin evolution process from two different spaces—the real space and
 367 the phase space, which provides a clear picture of spin dynamics in PFG diffusion experiments.

368 These two methods agree with each other. They get the same PFG signal attenuation equation,
 369 (11) or (16), which can be solved by the Adomian decomposition method. The solution gives PFG
 370 signal attenuation expressions (21a)-(21c), which include the finite gradient pulse width effect.
 371 Understanding the FGPW effect is important as the clinical MRI applications often use long gradient
 372 pulse. Additionally, using long gradient pulses allows researchers to monitor slower diffusion in
 373 polymer or biological systems where the molecules or ions often diffuse slowly. The consistent results
 374 from two different methods help us better understand the FGPW effect.

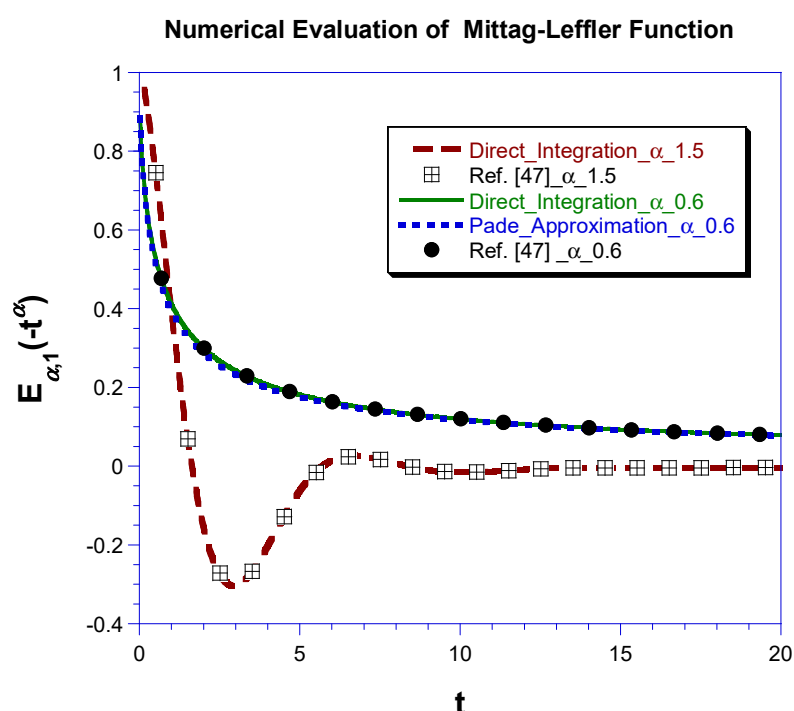
375 Additionally, the two methods agree with other methods. First, the PFG signal attenuation
 376 equation (17) obtained here is the same as that obtained by the integral modified-Bloch equation
 377 method [29]. Second, the results agree with the CTRW simulation as shown in Figure 2. In Figure
 378 2a, the fractional diffusion constant $D_f = 6.6 \times 10^{-11} \text{ m}^\beta/\text{s}^\alpha$ was obtained from fitting the curve of mean
 379 square displacement versus t by equation $\langle |z|^\beta \rangle = 2D_f t^\alpha / \Gamma(1 + \alpha)$. Figure 2b shows the PFG signal
 380 attenuation of anomalous diffusion obtained by Equations (22a-c) based on the Adomian
 381 decomposition method, Equation (32) based on the direct integration method, and the CTRW
 382 simulation. Other parameters used in Figure 2 are $\alpha = 0.5, \beta = 2, g = 0.1 \text{ T/m}$, $\Delta - \delta$ equaling 0 ms,
 383 20 ms. Interested readers can be referred to [29] for additional comparison between the theoretical
 384 prediction and the CTRW simulation. Third, the PFG signal attenuation expressions (22 a-c) are
 385 also consistent with those obtained by various approximation methods such as the non-Gaussian
 386 phase distribution (nGPD) method [26], and instantaneous signal attenuation method [25]. The
 387 same SGP approximation results, Equation (23) can be obtained by all these five different methods:
 388 the EPSDE method [17], the instantaneous signal attenuation method [25], the nGPD method [26],
 389 the method to observe the signal intensity at the origin, and the modified-Bloch equation method
 390 [29]. Moreover, Equation (27), $S(t) \approx E_{\alpha,1} \left(- \int_0^t D_f K^\beta(t') dt'^\alpha \right)$ can be approximately obtained in this
 391 paper, which agrees with that obtained from the instantaneous signal attenuation method [25].



392
 393 **Figure 2.** Comparison of the PFG signal attenuation from theoretical predictions with CTRW
 394 simulation: (a) mean square displacement from CTRW simulation, (b) PFG signal attenuation from
 395 different methods: the Adomian decomposition method with Equations (22a-c), the direct integration
 396 method with Equation (32), the and the CTRW simulation. The parameters used are $\alpha = 0.5, \beta = 2$,
 397 $D_f = 6.6 \times 10^{-11} \text{ m}^\beta/\text{s}^\alpha$, and $g = 0.1 \text{ T/m}$.

398
 399 The numerical evaluation of PFG signal attenuation by Equation (20) or (30) can be conveniently
 400 performed by the direct integration method. Figure 2b shows that the results of the direct integration
 401 method agree with that obtained from the Adomian decomposition method. Compared to the
 402 Adomian decomposition method, the computing speed of the direct integration method improves by

403 orders of magnitudes. The speed improvement is because in the direct integration method, each
 404 $S(t_j)$ in Equation (32) is only a single time integration, while in the Adomian decomposition method,
 405 $S(t_j) = \sum_{n=0}^{\infty} S_n(t_j)$ is a superposition of many terms of time integration. Additionally, from Equations
 406 (33) and (34), the direct integration method can be used to calculate Mittag-Leffler type functions and
 407 their derivative. Figure 3 shows that the Mittag-Leffler function (MLF) calculated from the direct
 408 integration method agree with that calculated by other methods in [47,48]. The Pade approximation
 409 method in [48] is only for subdiffusion. Because the direct integration method does not cause
 410 overflow, which can be a useful method to calculate Mittag-Leffler type functions. The Fortran code
 411 for MLF calculation can be obtained from the link: [https://github.com/GLin2017/Mittag-Leffler-](https://github.com/GLin2017/Mittag-Leffler-function-calculated-by-Direct-Integration)
 412 [function-calculated-by-Direct-Integration](https://github.com/GLin2017/Mittag-Leffler-function-calculated-by-Direct-Integration). This direct integration method will be a great help to the
 413 application of current theoretical results to PFG anomalous diffusion in NMR and MRI.



414
 415 **Figure 3.** Comparing the MLF calculated by different methods: Equation (33) from the direct
 416 integration method, the Pade approximation method [48], and the method used in [47].

417
 418 In the current results, only PFG anomalous diffusion of single quantum coherence is considered.
 419 The results here can be easily extended to handle PFG anomalous diffusion of intramolecular
 420 multiple quantum coherence (MQC) [26,38]. As the gradient field induced phase evolution of an n
 421 order intramolecular MQC is n times faster than the corresponding single quantum coherence, the
 422 PFG signal attenuation of intramolecular MQC is the same as that of single quantum coherence with
 423 an effective gradient intensity ng [40]. Therefore, for intramolecular MQC in PGSE or PGSTE
 424 experiments, the PFG signal attenuation equation is

$$425 \quad S(t) = \sum_{k=0}^{m-1} S^{(k)}(0^+) \frac{t^k}{k!} + J^\alpha (a_{MQC}(t)S(t)), m-1 < \alpha < m, \quad (35)$$

426 where

$$427 \quad a_{MQC}(t) = -K_{MQC}^\beta(t) D_{f_2} = \begin{cases} -n^\beta (\gamma g t)^\beta D_f, & 0 < t \leq \delta \\ -n^\beta (\gamma g \delta)^\beta D_f, & \delta < t \leq \Delta \\ -n^\beta (\gamma g)^\beta (\Delta + \delta - t)^\beta D_f, & \Delta < t \leq \Delta + \delta \end{cases}. \quad (36)$$

428 From Equation (36), it is obvious that the $a_{MQC}(t)$ in the MQC equals $n^\beta a(t)$.

429 This paper only considers the spin self-diffusion that can be described by the time-space
 430 fractional diffusion equation based on the fractional derivative. In general, the two methods used in
 431 this paper can be applied to other types of anomalous diffusions such as that described by the time-
 432 space diffusion equation based on the fractal derivative [49], etc. Additionally, only the symmetric
 433 anomalous diffusion in homogeneous spin systems is studied here. In real applications, the
 434 anomalous diffusion can take place in complicated systems such as inhomogeneous system,
 435 restricted geometries [27], anisotropic system [42], non-symmetric system, etc. Additionally, the
 436 gradient field may be nonlinear [50]. The current methods may face challenges in these complicated
 437 situations, which reminds us that much effort is required to the studying of PFG anomalous diffusion.
 438

439 **Conflicts of Interest:** the authors declare no conflict of interest.

440 Appendix A: Definition of the fractional derivative.

441 The definition of the space fractional derivative [5,30-32] is given by

$$442 \frac{d^\beta}{d|z|^\beta} = -\frac{1}{2 \cos \frac{\pi\alpha}{2}} \left[{}_{-\infty}D_z^\beta + {}_zD_\infty^\beta \right], \quad (\text{A.1})$$

443 where

$$444 {}_{-\infty}D_z^\beta f(z) = \frac{1}{\Gamma(m-\beta)} \frac{d^m}{dz^m} \int_{-\infty}^z \frac{f(y)dy}{(z-y)^{\beta+1-m}}, \beta > 0, m-1 < \beta < m, \quad (\text{A.2})$$

445 and

$$446 {}_zD_\infty^\beta f(z) = \frac{(-1)^m}{\Gamma(m-\beta)} \frac{d^m}{dz^m} \int_z^\infty \frac{f(y)dy}{(y-z)^{\beta+1-m}}, \beta > 0, m-1 < \beta < m. \quad (\text{A.3})$$

447 References

1. Wyss, W.; *J. Math. Phys.* **1986**, 2782-2785.
2. Metzler, R.; Klafter, J. The random walk's guide to anomalous diffusion: a fractional dynamics approach. *Phys. Rep.* **2000**, 339, 1-77.
3. Sokolov, I.M. Models of anomalous diffusion in crowded environments. *Soft Matter* **2012**, 8, 9043-9052.
4. Kopf, M.; Corinth, C.; Haferkamp, O.; Nonnenmacher, T.F. Anomalous diffusion of water in biological tissues. *Biophys. J.* **1996**, 70, 2950-2958.
5. Saichev, A.I.; Zaslavsky, G.M. Fractional kinetic equations: solutions and applications. *Chaos* **1997**, 7(4), 753-764.
6. Lindsey, C.P.; Patterson, G.D. Detailed comparison of the Williams-Watts and Cole-Davidson functions. *J. Chem. Phys.* **1980**, 73, 3348-3357.
7. Kaplan, J.I.; Garroway, A.N. Homogeneous and inhomogeneous distributions of correlation times. Lineshapes for chemical exchange. *J. Magn. Reson.* **1982**, 49, 464-475.
8. Hahn, E.L. Spin echoes. *Phys. Rev.* **1950**, 80, 580-594.
9. Torrey, H. C. Bloch Equations with Diffusion Terms. *Phys. Rev.* **1956**, 104(3), 563-565.
10. McCall, D. W.; Douglass, D. C.; Anderson, E. W.; Bunsenges, B. *Physik. Chem.* **1963**, 67, 336-340.
11. Stejskal, E. O.; Tanner, J. E. *J. Chem. Phys.* **1965**, 42, 288-292; doi: 10.1063/1.1695690.
12. Price, W.S. Pulsed-field gradient nuclear magnetic resonance as a tool for studying translational diffusion: Part 1. Basic theory. *Concepts Magn. Reson.* **1997**, 9, 299.

13. Price, W.S.; *NMR Studies of Translational Motion: Principles and Applications*; Cambridge University Press, 2009.
14. Callaghan, P. *Translational Dynamics and Magnetic Resonance: Principles of Pulsed Gradient Spin Echo NMR*; Oxford University Press, 2011.
15. McRobbie, D. W.; Moore, E. A.; Graves, M. J.; Prince, M. R. *MRI From Picture to Proton*; 2nd ed. Cambridge, England: Cambridge University Press; 2007; p. 338.
16. Magin, R.L.; Abdullah, O.; Baleanu, D.; Zhou, X.J. Anomalous diffusion expressed through fractional order differential operators in the Bloch–Torrey equation. *J. Magn. Reson.* **2008**, *190*, 255–270.
17. Lin, G. An effective phase shift diffusion equation method for analysis of PFG normal and fractional diffusions. *J. Magn. Reson.* **2015**, *259*, 232–240.
18. Kärger, J.; Pfeifer, H.; Vojta, G. Time correlation during anomalous diffusion in fractal systems and signal attenuation in NMR field-gradient spectroscopy. *Phys. Rev. A* **1988**, *37*(11), 4514–4517.
19. Kimmich, R. *NMR: Tomography, Diffusometry, Relaxometry*; Springer-Verlag, Heidelberg, 1997.
20. Fatkullin, N.; Kimmich, R. Theory of field-gradient NMR diffusometry of polymer segment displacements in the tube-reptation model. *Phys. Rev. E* **1995**, *52*, 3273–3276.
21. Bennett, K.M.; Schmainda, K.M.; Bennett, R.T.; Rowe, D.B.; Lu, H.; Hyde, J.S. Characterization of continuously distributed cortical water diffusion rates with a stretched-exponential model. *Magn. Reson. Med.* **2003**, *50*, 727–734.
22. Bennett, K.M.; Hyde, J.S.; Schmainda, K.M. Water diffusion heterogeneity index in the human brain is insensitive to the orientation of applied magnetic field gradients. *Magn. Reson. Med.* **2006**, *56*, 235–239.
23. Klafter, J.; Sokolov, I.M. *First step in random walk. From Tools to Applications*; Oxford University Press, New York, 2011.
24. Hanyga; Seredyńska, M. Anisotropy in high-resolution diffusion-weighted MRI and anomalous diffusion. *J. Magn. Reson.* **2012**, *220*, 85–93.
25. Lin, G. Instantaneous signal attenuation method for analysis of PFG fractional diffusions. *J. Magn. Reson.* **2016**, *269*, 36–49.
26. Lin, G. Analyzing signal attenuation in PFG anomalous diffusion via a non-gaussian phase distribution approximation approach by fractional derivatives. *J. Chem. Phys.* **2016**, *145*, 194202.
27. Lin, G.; Zheng, S.; Liao, X. Signal attenuation of PFG restricted anomalous diffusions in plate, sphere, and cylinder. *J. Magn. Reson.* **2016**, *272*, 25–36.
28. Damion, R.A.; Packer, K.J. Predictions for pulsed-field-gradient NMR experiments of diffusion in fractal spaces. *Proc.: Math., Phys. Eng. Sci.* **1997**, *453*, 205–211.
29. Lin, G. The exact PFG signal attenuation expression based on a fractional integral modified-Bloch equation, arXiv:1706.02026; Lin, G. Fractional differential and fractional integral modified-Bloch equations for PFG anomalous diffusion and their general solutions, [arXiv:1702.07116](https://arxiv.org/abs/1702.07116).
30. Mainardi, F.; Luchko Yu.; Pagnini, G. The fundamental solution of the space-time-fractional diffusion equation. *Fract. Calc. Appl. Anal.* **2001**, *4*, 153–192.
31. Gorenflo, R.; Mainardi, F. Fractional Diffusion Processes: Probability Distributions and Continuous Time Random Walk. *Springer Lecture Notes in Physics*, No 621, Berlin, 2003, pp. 148–166.
32. Balescu, R. V-Langevin equations, continuous time random walks and fractional diffusion. *Chaos, Solitons and Fract.* **2007**, *34*, 62–80.

33. Mittal, R. C.; Nigam, R. Solution of fractional integro-differential equations by Adomian decomposition method. *Int. J. of Appl. Math. and Mech.* **2008**, *4*(2), 87-94.
34. Adomian, G. *Solving Frontier Problems of Physics: The Decomposition Method*; Kluwer Academic, Dordrecht, 1994.
35. Adomian, G.; Rach, R. Inversion of nonlinear stochastic operators. *J. Math. Anal. Appl.* **1983**, *91*, 39-46.
36. Adomian, G. On the solution of algebraic equations by the decomposition method. *J. Math. Anal. and Appl.* **1985**, *105*, 141-166.
37. Duan, J.-S.; Rach, R.; Baleanu, D.; Wazwaz, A.-M. A review of the Adomian decomposition method and its applications to fractional differential equations. *Commun. Frac. Calc.* **2012**, *3* (2), 73-99.
38. Grinberg, F.; Farrher, E.; Ciobanu, L.; Geffroy, F.; Bihan, D. Le; Shah, N.J.; Non-gaussian diffusion imaging for enhanced contrast of brain tissue affected by ischemic stroke. *PLoS ONE* **2014**, *9*(2), e89225
39. Zax, D.; Pines, A. *J. Chem. Phys.* **1983**, *78*(10), 6333.
40. Karlicek Jr., R.F.; Lowe, I.J. A modified pulsed gradient technique for measuring diffusion in the presence of large background gradients. *J. Magn. Reson.* **1980**, *37*(1), 75-91.
41. Kilbas, A.A.; Saigo, M. Solutions of integral equation of Abel-Volterra type, *Diff. Integr. Equations* **1995**, *8*, 993-1011.
42. Lin, G. General PFG signal attenuation expressions for anisotropic anomalous diffusion by modified-Bloch equations, arXiv:1706.06552v2.
43. Germano, G.; Politi, M.; Scalas, E.; Schilling, R.L. *Phys. Rev. E* **2009**, *79*, 066102.
44. Cicerone, M. T. Wagner, P. A. Ediger, M. D. Translational Diffusion on Heterogeneous Lattices: A Model for Dynamics in Glass Forming Materials. *J. Phys. Chem. B* **1997**, *101*, 8727.
45. Lin, G.; Zhang, J.; Cao, H.; Jones, A. A. *J. Phys. Chem. B* **2003**, *107*, 6179.
46. Lin, G.; Aucoin, D.; Giotto, M.; Canfield, A.; Wen, W.; Jones, A.A. *Macromolecules* **2007**, *40*, 1521.
47. Gorenflo, R.; Loutchko, J.; Luchko, Y. Computation of the Mittag-Leffler function $E_{\alpha,\beta}(z)$ and its derivative. *Fract. Calc. Appl. Anal.* **2002**, *5*, 491-518.
48. Zeng, C.; Chen, Y. Global Pade approximations of the generalized Mittag-Leffler function and its inverse. *Fract. Calc. Appl. Anal.* **2015**, *18*, 1492-1506.
49. Chen, W.; Sun, H.; Zhang, X.; Korošak, D. Anomalous diffusion modeling by fractal and fractional derivatives, *Comput. Math. Appl.* **2010**, *59*(5), 1754-1758.
50. Doussal, P. Le; Sen, P.N. Decay of nuclear magnetization by diffusion in a parabolic magnetic field: an exactly solvable model. *Phys. Rev. B* **1992**, *46*, 3465-3485.